











Research Article

Dental Biopolymer Composites with Antibiotics, Bisphosphonate, and Hydroxyapatite for Possible Use in Bone Tissue Regeneration

Mihaela Maria Budiul ¹, **Gabriela Vlase** ¹, **Daniel Negru**,^{2,3,4} **Dorinel Okolišan**,¹ **Ionela-Amalia Bradu** ¹, **Alexandra Tășală**,¹ **Alexandru Pahomi** ¹, **Titus Vlase** ¹, **Daniela Jumanca** ^{2,3,4}, **Atena Galuscan**,^{2,3,4} **Paula Sfirloaga** ⁵, **Nicoleta Carabă** ⁶, **Roxana Popescu** ⁷ and **Anamaria Matichescu** ^{2,3,4}

¹Research Centre for Thermal Analysis in Environmental Problems- ICAM, West University of Timisoara, Pestalozzi Street 16, Timisoara 300115, Romania

²University of Medicine and Pharmacy “Victor Babes”, Faculty of Dental Medicine, Timisoara, Romania

³Department of Preventive Dentistry, Community and Oral Health, Spl. Tudor Vladimirescu No. 14A, Timisoara 300173, Romania

⁴Translational and Experimental Clinical Research Center in Oral Health (TEXC-OH), 14A Tudor Vladimirescu Ave., Timisoara 300173, Romania

⁵National Institute for Research and Development in Electrochemistry and Condensed Matter, Str. Dr. A. Paunescu Podeanu, Nr. 144, Timișoara 300569, Romania

⁶West University of Timisoara, Faculty of Chemistry, Biology, Geography, Department of Biology-Chemistry, Pestalozzi Street 16, Timisoara 300115, Romania

⁷Faculty of Medicine, University of Medicine and Pharmacy “Victor Babeș”, Cell and Molecular Biology Department, Tudor Vladimirescu 14, Timisoara 300041, Romania

Correspondence should be addressed to Gabriela Vlase; gabriela.vlase@e-uvt.ro

Mihaela Maria Budiul and Daniel Negru contributed equally to this work.

Received 10 July 2023; Revised 11 December 2023; Accepted 31 December 2023; Published 22 January 2024

Academic Editor: Ajaya Kumar Singh

Copyright © 2024 Mihaela Maria Budiul et al. This is an open access article distributed under the Creative Commons Attribution License, which permits unrestricted use, distribution, and reproduction in any medium, provided the original work is properly cited.

The aim of the present study was to formulate new variants of synthetic and animal-source bone materials coated with different biopolymers, containing antibiotics (ampicillin and oxacillin) and alendronate drugs. Validation consists in establishing mixtures that do not present interactions between components. These materials should act as a drug delivery system alongside the bone base. Natural polymers such as chitosan, alginate, and kappa-carrageenan have been shown to be optimal materials for drug delivery due to their intrinsic biocompatibility. Binary, ternary, and quaternary mixtures between components are analyzed by FT-IR spectroscopy, UV-Vis analysis, thermogravimetry (TGA), and scanning electron microscopy (SEM). The analysis led to the validation of materials suitable for the controlled release of active substances, which have the greatest chance of increasing the speed of bone regeneration, as well as helping in the local administration of antibiotics, which currently must be administered in the form of oral formulations or an injection. According to the FTIR, thermogravimetry, UV-Vis, SEM, and cytotoxicity tests performed in this study, it can be said that it is quite easy to obtain materials that can be used in dental practice that facilitate bone reconstruction through local treatment. At the same time, it was found that both active substances can be incorporated into the material together with Alg and Chit, thus limiting the adverse effects and maximizing the local beneficial effects.

1. Introduction

The goal of modern periodontal therapy has always been to eliminate the infection and restore the periodontal bone defect. Bone-grafting procedures have been used to regenerate bone within osseous defects, including that of the alveolar bone.

Synthetic bone grafts and bone grafts of animal origin are only osteoconductive scaffolds that guide the formation of new bone into the osseous defect [1]. Therefore, bone grafting materials need to be developed with different drugs that can be released at the right site, which means shortening the administration time and avoiding toxicity to other organs.

This study aims to formulate synthetic and animal-derived bone materials with different components, containing antibiotics (Ampi and Oxa) and alendronate drugs. These materials should act as a system for transmucosal drug delivery. Drug delivery systems, such as those based on polymers, can be designed to enhance the pharmacological and therapeutic properties of topically administered drugs [2]. A preprint of this study has previously been published [3]. To date, our research team has published other preliminary studies on drug delivery systems and compatibility studies of active ingredients with various pharmaceutical excipients [4, 5].

In this study, we chose to introduce into the composition of commonly used bone that restores the lost jaw structure and various other substances that have a beneficial role in stimulating bone regeneration and preventing necrosis and infection at this level. Before and after periodontal surgery or bone reconstruction of the oral cavity, the patient must receive prophylactic antibiotics to prevent infections. Depending on the severity of the procedure, this treatment may last for a longer period, as oral or injectable administration of antibiotics has its drawbacks (large quantity of antibiotic to be administered, appearance of candidiasis albicans, allergies, digestive problems, and complications at the injection site). The possibility of incorporating small quantities of antibiotics directly into bone reconstruction materials, which can be gradually released at the site of the operation, will eliminate the drawbacks of the classical administration of antibiotics.

In the oral cavity live over 600 different microbial species, which under favorable conditions overgrow, so any intervention at this level involves the risk of infection. The main species that develop in the oral cavity in case of improper hygiene are streptococci and staphylococci. The two bone replacement materials used in this study are presented in the literature as materials with satisfactory cytocompatibility, with viability >70% [6, 7]. These materials are currently used in the dental office in current practice without cytotoxic reactions or local cell proliferation being reported. To avoid drug-associated complications, natural polymers such as chitosan, alginate, and kappa-carrageenan have been shown to be optimal materials in the field of drug delivery due to their intrinsic biocompatibility [8]. Chitosan (Chit) has been extensively studied in the development of controlled release drug delivery systems because it facilitates the

transmucosal absorption of drugs because the electrostatic interaction with the negatively charged mucosal surface is due to its positive charges [2]. Kappa-carrageenan (Car) is another natural polymer that is believed to have antimicrobial, anticoagulant, and antioxidant activity [9]. Alginate (Alg) is a nontoxic polymer that is biodegradable and has mucoadhesive properties [10]. According to the literature, through the local administration of antibiotics, the probability of developing antibiotic resistance is lower. However, by using a low dose of antibiotics, we obtain the same release time [11].

Hybrid hydrogels composed of chitosan and alginate have demonstrated great potential in bone tissue engineering and regeneration. In this work, we took into account the favorable characteristics of chitosan and alginate to design new nanocomposites for the regeneration of bone tissue, namely, the fact that the results of *in vitro* biological tests performed on osteoblastic present in literature cell cultures demonstrated the great biocompatibility of hybrid materials that have a polymeric base the two biopolymers [12–18]. Soft biomaterials such as hydrogels may have the potentialities to serve as a cell-encapsulating matrix [19, 20].

Ampicillin (Ampi or -aminobenzylpenicillin or 6-[d(-)-aminophenylacetamido] penicillanic acid is an antibiotic of the penicillin class with a beta-lactamic structure and is classified as a broad-spectrum beta-lactam antibiotic that has bactericidal activity [21, 22]. Among antibiotics, we chose ampicillin since it is a common antibiotic prescribed by dentists because it has broad-spectrum action. Ampicillin belongs to the group of drugs known as beta-lactam broad-spectrum penicillin [23]. It is a semisynthetic derivative of penicillin and is active against Gram-positive cocci, including streptococci, staphylococci, and enterococci species not resistant to penicillin. It displays activity against Gram-negative organisms, Gram-positive anaerobic organisms, and Gram-negative anaerobic organisms. Ampicillin also has activity against certain spirochetes [24]. Penicillin antibiotics are also common forms recommended for dental infections. Ampicillin is indicated in infections caused by sensitive bacteria located in the respiratory, ENT, urogenital, and digestive tracts.

Oxacillin (Oxa) is a drug of the beta-lactam antibiotic class, beta-lactamase-resistant penicillins used in the treatment of infections caused by Staphylococci and Streptococci sensitive to oxacillin: respiratory tract infections, otorhinolaryngological infections, skin infections, and bone infections. The combination of the two types of antibiotics offers a broader spectrum of protection both from a periodontal and bone point of view, and in the future, other types of antibiotics and their combination with metronidazole may be included in further studies [25].

Bisphosphonates are a group of drugs commonly used to treat various bone diseases, including osteoporosis, malignant hypercalcemia, or Paget's disease. Alendronate (Alen or [(4-amino-1-hydroxybutylidene)-bisphosphonate] trihydrate [26] is an amino bisphosphonate that significantly improves bone density and mass in the treatment of periodontal defects [27]. Alen has an affinity for calcium phosphate and binds tightly to hydroxyapatite [28].

Bisphosphonates are a class of pharmaceuticals applied as treatment for several bone disorders and cancers, such as Paget's disease, osteoporosis, multiple myeloma, and hypercalcemia of malignancy, that act by suppressing osteoclast differentiation, impairing its activity, and leading to early apoptosis. Their activity on osteoclast is also related to adverse events as damaged bone healing and remodeling processes that have as a consequence an augmented risk of developing osteonecrosis of jaw, a serious and debilitating condition, in patients subjected to surgical dental procedures as extraction or implant placement [29–35].

The new synthesized materials containing Bio-Oss, antibiotics, bisphosphonate, and biopolymer would have the advantage of local treatment and prevention of an infection, as well as bone reconstruction with the advantages of a local administration with a minimum amount of active substance.

Local delivery methods have been used to reduce or to avoid the possibility of adverse systemic effect [36], so the objective of our study is to obtain the best biopolymer composites with penicillin-class antibiotics and Alen. During the obtaining new bone-grafting materials, it is very important to know the physicochemical properties of drugs and the individual components. The studies presented in the literature prove that thermal analysis techniques are methods used for the physicochemical characterization of various materials used in pharmaceutical and other fields [37–47]. In the present paper, by combining the complementary physicochemical techniques, TG/DTG/HF, FTIR-UATR, UV-Vis ultraviolet-visible, and SEM-EDX, it is determined which is the best bone-grafting material that can be used to release the analyzed active ingredients individually and in the form of a mixture.

The purpose of this study is the physicochemical validation of mixtures that do not exhibit interactions between components. This is the necessary first step in the case of studies of new materials or pharmaceutical formulations. The presented study succeeds in establishing by combining the results of several complementary physicochemical techniques (TG, FTIR, SEM-scanning electron microscopy, and UV-Vis ultraviolet-visible), which would be the best variant of material that presents the active substances intact, and thus, it can be tested *in vitro* or *in vivo* for medical use.

2. Materials and Methods

The biopolymers used were purchased as follows: chitosan from Acros Organics, CAS number: 9012-76-4, κ -carrageenan (Car) from Acros Organics, CAS number: 11114-20-8 and alginate from Sigma Aldrich P.N. (Saint Louis, MO, USA, W201502).

The antibiotics used were purchased as follows: ampicillin (see Figure 1(a)) from Antibiotice Iasi and oxacillin (see Figure 1(b)) from Antibiotice Iasi.

The active substance, alendronate sodium (see Figure 1(c)), was purchased from Sigma, Lot no. LRAC6414, CAS-No. 121268-17-5, USA. Bone graft materials were purchased as follows: synthetic bone grafts BOS-BioOSS Sint, Maxresorb, Lot 1956-2, and Botiss biomaterials and bone grafts of animal origin BON-BioOSS Nat, cerabone,

a natural bovine bone from Botiss biomaterials, Lot 20KA10720, particle size: 0.5–1 mm. Both materials were produced by Botis-biomaterials GmbH and were distributed by MegaGen dental implant SRL. București, România.

For the compatibility studies of the active substances with each component of the new release systems, obtaining mixtures was considered. The processes and stages that occur during the synthesis of bone graft materials were followed, and then the integrity of the active substances in the mixtures was verified.

2.1. Sample Preparation. Three sets of samples were prepared. The first set of samples consists of the binary mixture of the active ingredients (antibiotics and alendronate) and the components of the final material, in a mass ratio of 1 : 1, to highlight the possible interactions that may occur. The second set contained three components, namely, an antibiotic, Alen, and the biopolymer. The last set of samples contained the active components, the biopolymer, and the calcium source represented by bone (natural or synthetic) in a mass ratio of 1 : 1 : 2 : 3. The study was carried out in stages since in mixtures of three components, the influence of water (introduced with the biopolymer) is added, which can facilitate the interactions between the components. In the framework of the current studies of the new pharmaceutical formulations, stress studies are carried out that provide for the realization of the studies by analyzing the binary mixtures both in the ascended form and with a minimum of 5% moisture and compared with the individual substances [42, 44]. The study of the last set of samples aims to validate the material from the point of view of the absence of interactions between the active substances used. The mixtures and their notations are presented in Table 1 binary mixture; Table 2 ternary mixture; and Table 3 quaternary mixture.

The following procedure was used to prepare the biopolymer solutions: sodium alginate was dissolved in water (1.5 g/L), through stirring by using a magnetic stirrer, for 2 hours at room temperature. Chitosan solution was prepared by dissolving chitosan in acetic acid 5% under continuous stirring at room temperature for 8 hours, and the last solution was prepared by dissolving carrageenan (2 g/L) in water with vigorous stirring at room temperature. These solutions were then used to obtain tertiary and quaternary mixtures.

Samples were obtained by mixing and homogenizing the components, then dried in an oven for 8 hours at room temperature in dried atmosphere, and stored in sterile Eppendorf bottles and in sterile multiwall plates until analysis.

2.2. FTIR Analysis. FTIR data were obtained on a Shimadzu AIM-9000 with ATR after 20 recordings at a resolution of 4 cm^{-1} in the range of $4000\text{--}400\text{ cm}^{-1}$.

2.2.1. Thermogravimetric Analysis. The thermal behavior was determined using an aluminum crucible on TG/DTA DIAMOND Thermal Analyzer produced by Perkin Elmer. Analyses were performed in a dynamic air atmosphere

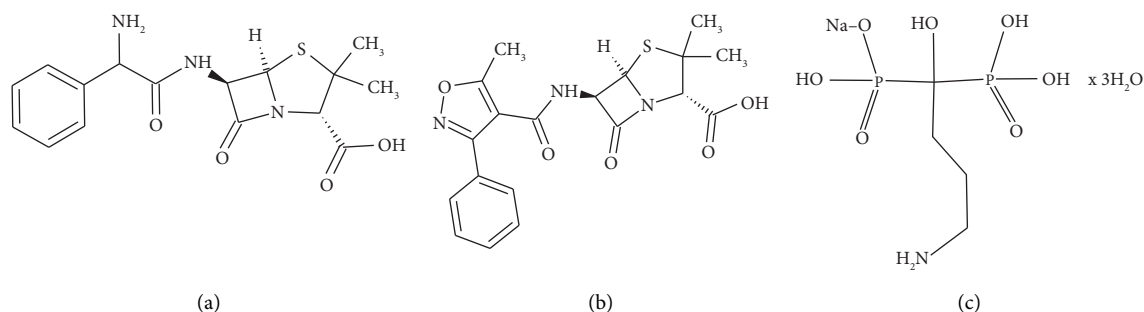


FIGURE 1: (a) Chemical structure of Ampicillin. (b) Chemical structure of Oxacillin. (c) Chemical structure of Alendronate.

TABLE 1: Binary mixture.

Samples	Composition mass report
Oxa_Alen	1:1
Ampi_Alen	1:1
Oxa_Chit	1:1
Ampi_Chit	1:1
Alen_Chit	1:1
Oxa_Alg	1:1
Ampi_Alg	1:1
Alen_Alg	1:1
Oxa_Car	1:1
Ampi_Car	1:1
Alen_Car	1:1

TABLE 2: Ternary mixture.

Samples	Composition mass report
Oxa_Alen_Chit	1:1:2
Ampi_Alen_Chit	1:1:2
Oxa_Alen_Car	1:1:2
Ampi_Alen_Car	1:1:2
Oxa_Alen_Alg	1:1:2
Ampi_Alen_Alg	1:1:2

TABLE 3: Quaternary mixture.

Samples	Composition mass report
Oxa_Alen_Chit_BON	1:1:2:3
Oxa_Alen_Chit_BOS	1:1:2:3
Ampi_Alen_Chit_BON	1:1:2:3
Ampi_Alen_Chit_BOS	1:1:2:3
Oxa_Alen_Car_BON	1:1:2:3
Oxa_Alen_Car_BOS	1:1:2:3
Ampi_Alen_Car_BON	1:1:2:3
Ampi_Alen_Car_BOS	1:1:2:3
Oxa_Alen_Alg_BON	1:1:2:3
Oxa_Alen_Alg_BOS	1:1:2:3
Ampi_Alen_Alg_BON	1:1:2:3
Ampi_Alen_Alg_BOS	1:1:2:3

(synthetic air 5.0 Linde Gas with flow $100 \text{ mL} \cdot \text{min}^{-1}$) at a heating rate, $\beta = 10^\circ\text{C} \cdot \text{min}^{-1}$, in the temperature range of 30–500°C for the two antibiotics and alendronate and for the

binary mixtures. All analyzed samples had a mass between 8 and 12 mg.

2.2.2. UV-Vis Spectrophotometry. To obtain the UV-Vis spectra, a UV-Vis T90+ spectrophotometer with a double beam in the photometric range 190–900 nm was used. All absorbance measurements were performed at room temperature using distilled water as a blank in a 10 mm UV/Vis spectroscopy cell. Comparative studies of the standards of active substances with solutions obtained by maintaining the synthesized materials for one hour in distilled water at room temperature were carried out. The studies were conducted for qualitative purposes. UV-Vis analyzes were performed only in the case of ternary mixtures because these are the materials that should be applied in dental practice.

SEM analysis was performed with the Inspect scanning electron microscope in low vacuum, at a pressure of 60 Pa and 30 kV voltage, and de EDS analysis was performed with the Jeol-JSM IT 200 electron microscope in low vacuum 80 Pa, landing voltage 15.0 kV, and magnification $\times 1600$.

2.3. Cytotoxicity/Biocompatibility Test. The MCF7 cell line was used for the cytotoxicity/biocompatibility assay. For the cell line MCF7, cells obtained from passage 5 were used and cultured in a special DMEM culture medium supplemented with 10% fetal bovine serum (FBS) and 1% antibiotic mixture (penicillin-streptomycin). Cells were cultured in T75 flasks, in an incubator at 37°C and 5% CO₂ atmosphere. The culture medium was changed regularly at 2-3 day intervals. After reaching 80% confluence, the cells were detached from the flasks by trypsinization. Cells were seeded at a concentration of 5×10^4 cells per well in 96-well plates in a volume of 100 μl growth medium. After 24 h incubation, the solutions of the test compounds were added at the established concentrations, taking into account that they contained an antibiotic component. When determining the concentrations of the tested solutions, it was taken into account that the maximum permissible concentration of the antibiotic compatible with optimal development of the cells in the culture is 1%. Serial dilutions were prepared for each compound studied, and the final tested concentrations were C1-1%, C2-0.500%, C3-0.250%, C4-0.125%; C5-0.0625%, and C6-0.03125%.

3. Results and Discussion

3.1. FTIR Analysis of Active Substances. The study begins with the FTIR study of the active substances, namely, the antibiotics (Ampi and Oxa) and the bisphosphonate (Alen), respectively, in their initial form to obtain the data that we can follow in the binary mixtures.

In the case of Ampi, whose FTIR spectrum is shown in Figure 2, the appearance of some characteristic peaks can confirm with certainty the class of compounds into which this active substance can be cataloged. Thus, the most intense peak of the FTIR spectrum, at 1581.62 cm^{-1} , is assigned to amide linkage group, due to the deformation of the N-H bond (amide band II). Since the studied antibiotic is a compound “rich” in nitrogen atoms, and therefore, for N-H bonds, the vibrations of this single bond must appear in the FTIR spectrum. Thus, although the “width” of the peak at $3000\text{--}3500\text{ cm}^{-1}$ is due to the O-H bond vibration from the carboxylic group and as is well known, it usually “covers” the N-H bond vibrations, and this time, the presence of N-H bonds is highlighted by the appearance of smaller peaks, as shoulders of the OH band, for N-H stretching vibrations of the linkage group (amide) and the stretching vibration of the N-H bond from the NH_2 group of the 1-phenylmethanamine moiety [48].

The other peaks that can be assigned to the molecular moieties of ampicillin are as follows: although very weak but still important is the peak attributed to the lactam ring, from 1251.80 cm^{-1} , also called amide band III; the peak at 3059.10 cm^{-1} is attributed to hydrogen bridges; the peak at 2972.30 cm^{-1} can be attributed both to the vibrations of the C-H bond of the two methyl radicals of the 4-thia-1-azobicyclo[3.2.0]heptane fragment as well as to some intramolecular hydrogen bonds; regarding the area of the fingerprint, it should be mentioned that, here, the characteristic peak of the skeletal vibration of β -lactam occurs, at 677.01 cm^{-1} , and the vibration of the C-S bond of the bicyclic fragment occurs at 889.18 cm^{-1} .

If we take a closer look at the molecular structure of Oxa (Figure 3), we can see that it is similar to that of Ampi, and it has the same linking group, the same conformation, and substitution of the lactam ring, and the only difference is the oxazole fragment attached to the benzene ring; in ampicillin, the aromatic ring is substituted by the α -amino acetic radical. In the case of Oxa, the most intense peak of its FTIR spectrum (Figure 3), appearing at 1585.48 cm^{-1} , is assigned to the amide band II. Looking more closely at the “aspect” of this peak, we can see that it has a lateral “shoulder” at 1610.56 cm^{-1} , often called the amide I band, which corresponds to the C=O stretching vibration of β -lactams. The peak at 1429.25 cm^{-1} is attributed to the skeletal vibration of a benzene ring ($\nu\text{ C=C}$ and $\nu\text{ C-H}$). A peak at 1336.66 cm^{-1} corresponds to the skeletal vibration of the oxazole fragment.

Alendronic acid (Alen), an organophosphorus compound, consisting of two different fragments, a linear aliphatic amine and two phosphonic fragments, shows peaks in its FTIR spectrum that can be assigned to these moieties (Figure 4). Thus, for the aliphatic chain, the stretching

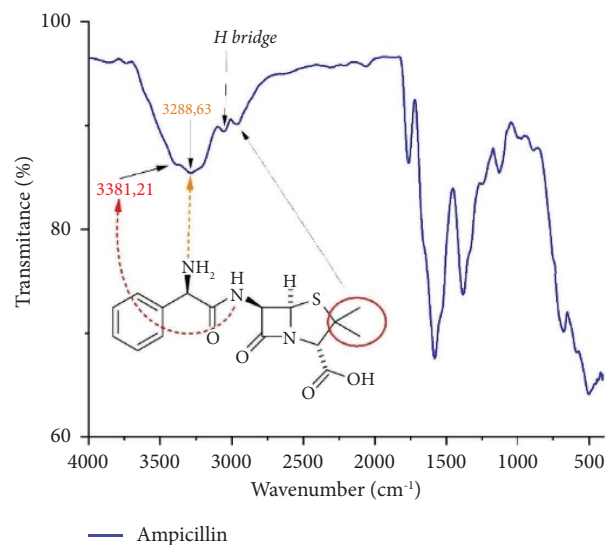


FIGURE 2: FTIR spectrum of ampicillin.

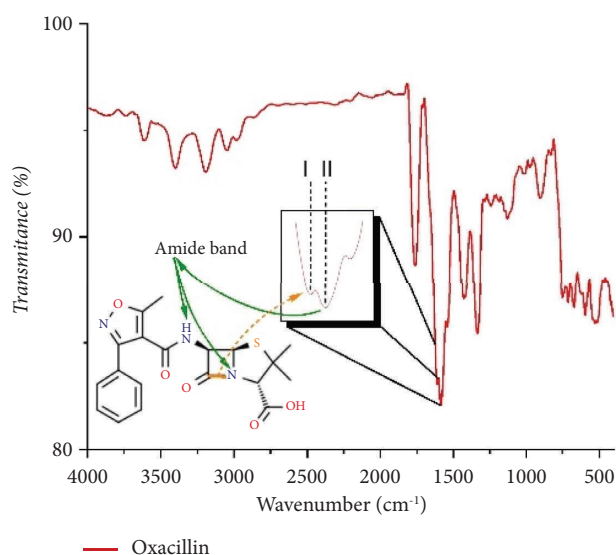


FIGURE 3: FTIR spectrum of oxacillin.

vibration of the N-H bond, from NH_2 , is located at 3476.66 cm^{-1} , and the stretching vibrations of the C-H bonds occur at 2948.08 cm^{-1} . For the hydroxylic groups, from the phosphonic moiety and the hydroxyl group of the carbon to which these phosphonic fragments are attached, the characteristic vibrations of the O-H bond are assigned to the peak at 3033.11 cm^{-1} . The peak from 1629.72 cm^{-1} is due to the asymmetric deformation of NH_3^+ , which means that the amino group of the aliphatic chain is protonated. Since alendronate incorporates phosphorus atoms into its structure, it exhibits the following peaks:

- (i) At 1138.00 cm^{-1} , for stretching vibrations of the two P=O bonds
- (ii) At 1035.77 cm^{-1} , for asymmetric stretching of the P-O bonds

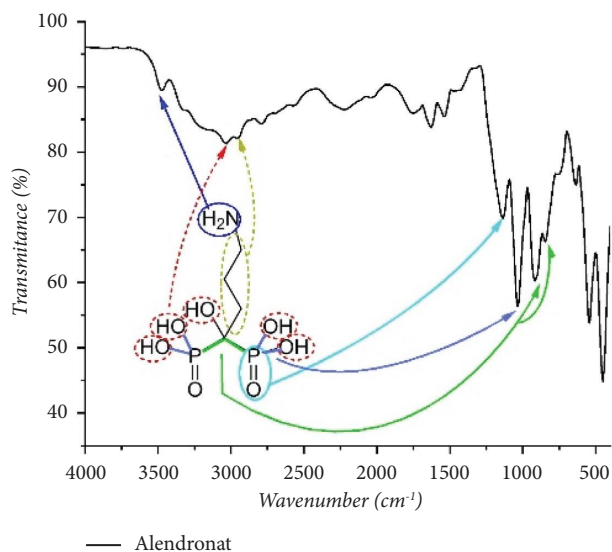


FIGURE 4: FTIR spectrum of Alen.

Both peaks, the one at 848.679 cm^{-1} and the one at 918.11 cm^{-1} , can be attributed to the asymmetric vibration of the -P-C- and -P-C-P- bonds.

3.1.1. FTIR Spectra of Active Substances in the Biopolymer Matrix. According to the synthesis method used to prepare biopolymer membranes and the attempt to incorporate antibiotics, we can say that the active substances are present in the obtained membranes, but FTIR analysis is still necessary in order to obtain a positive answer to their “physical” presence or absence in the polymer matrix. The assignment of peaks and their use as “witnesses” for the presence of active substances in the resulting membranes are discussed in more detail in the following subsections.

(1) Active Substance Incorporated in Alginate Membranes. The data obtained from the FTIR analysis are shown graphically in Figure 5(a). Thus, the broad peak from 3207.62 cm^{-1} is attributed to the stretching vibration of the O-H bonds. For the saccharide skeleton, the stretching vibrations of the C-H bonds appear at $\approx 2966\text{ cm}^{-1}$, while the $\nu\text{C-O}$ of the pyranose intrasaccharide bond has a peak at $\approx 1120.64\text{ cm}^{-1}$, a peak for $\nu\text{C-OH}$ at $\approx 1053.13\text{ cm}^{-1}$, and a peak in the fingerprint region that can be attributed to the -C-O-C- bond vibrations of the glycosidic linkages between the saccharide units.

In the case of Alen, the appearance of peaks for the stretching vibration of P=O bonds at 1313.52 cm^{-1} , asymmetric $\nu\text{P-C-P}$ at 835.17 cm^{-1} , and deformation vibrations of the hydroxyl groups attached to the phosphonic moiety at 1409.96 cm^{-1} confirms the nature of this antibiotic. According to Figure 5(b), the line denoting the amide band II trespasses the membrane with alendronate, even though this compound does not contain any amide nitrogen atom that could lead to its appearance. One explanation for the appearance of this peak, at 1602.84 cm^{-1} , is due to the asymmetric deformation of NH_3^+ , which means that the

terminal amino group of the aliphatic chain is somehow protonated. In addition, characteristic of the Amp_i_Alg and Oxa_Alg mixtures is the appearance of amide band I at 1666.49 cm^{-1} and amide band III at 1280.73 cm^{-1} , due to the presence of the lactam ring in antibiotics. Another peak characteristic only of these antibiotics is the peak at 1490.97 cm^{-1} which corresponds to $\nu\text{-C=C-}$ and $\nu\text{-C-H}$ (see Figure 5(b)).

In conclusion, we can say that the appearance of these peaks for the studied active substances, discussed above, indicates the presence of these medicinal compounds in the alginate mixtures.

(2) Active Substances Incorporated in κ -Carrageenan Membranes [4]. For κ -carrageenan membranes (Figure 6(a)), the characteristic peaks for the vibrations of the hydroxyl groups are located at 3290.55 cm^{-1} , while the vibrations of the C-H bonds in the saccharide units are present at 2953.32 cm^{-1} . For this polysaccharide, the vibrations of the pyranose units, more precisely the $\nu\text{C-O-C}$ bond vibrations of the pyranose ring, are located at 1141.85 cm^{-1} , of the C-OH bonds at 1047.34 cm^{-1} , and for the glycosidic bond, the $\nu\text{C-O-C}$ stretching vibrations are positioned at 916.18 cm^{-1} . Since the biopolymer is a sulfated galactan, at the wavenumber of 829.39 cm^{-1} , it shows a “fingerprint” due to $\nu\text{C-OSO}_3\text{H}$ and the absence of which would indicate a chemical modification of κ -carrageenan.

Regarding the active substances incorporated in the studied membranes (Figure 6(b)), three amide bands can be found for lactam antibiotics, as follows: amid band I at $\approx 1585\text{ cm}^{-1}$ due to $\nu\text{C=O}$, amide band II due to the N-H bending vibration of the amide linkage, and amide band III at $\approx 1230\text{ cm}^{-1}$ due to $\nu\text{C-N}$. Alendronate confirms its presence by means of $\nu\text{P=O}$ which appears at 1039.63 cm^{-1} , $\nu\text{P-OH}$ at 916.18 cm^{-1} , and $\nu\text{P-C-P}$ at 844.82 cm^{-1} [49].

(3) Active Substances Incorporated in Chitosan Membranes. The FTIR spectra of the binary mixtures of chitosan in which the three types of active substances were incorporated are represented in Figure 7(a). According to this figure, the peaks that can be attributed to the polymer matrix are as follows: the stretching vibrations of the OH bonds at 3211.47 cm^{-1} , the CH bonds at 2966.51 cm^{-1} , and the stretching vibrations of the N-H bonds at 3334.92 cm^{-1} , because the chitosan backbone has plenty of amino groups. Also attributed to chitosan are the peaks corresponding to the C-O stretching vibration of the pyranose ring at 1136.07 cm^{-1} , C-OH vibrations at 1053.13 cm^{-1} , vibrations for the glycosidic bond at 904.61 cm^{-1} , and also the vibration of the deformation of the N-H bond at 709.80 cm^{-1} [48–51].

As in the case of the other obtained mixtures (based on alginate and carrageenan), the successful incorporation of the active substances can be highlighted by the appearance of peaks that can prove their presence in the polymer matrix. Thus, according to the FTIR spectra presented in Figure 7(b), in addition to the vibrations of some bonds originating from chitosan, one can observe the following.

In the case of Amp_i and Oxa, lactam antibiotics, the appearance of amide bands I, II, and III is directly associated with the lactam ring, which can be an indisputable testimony

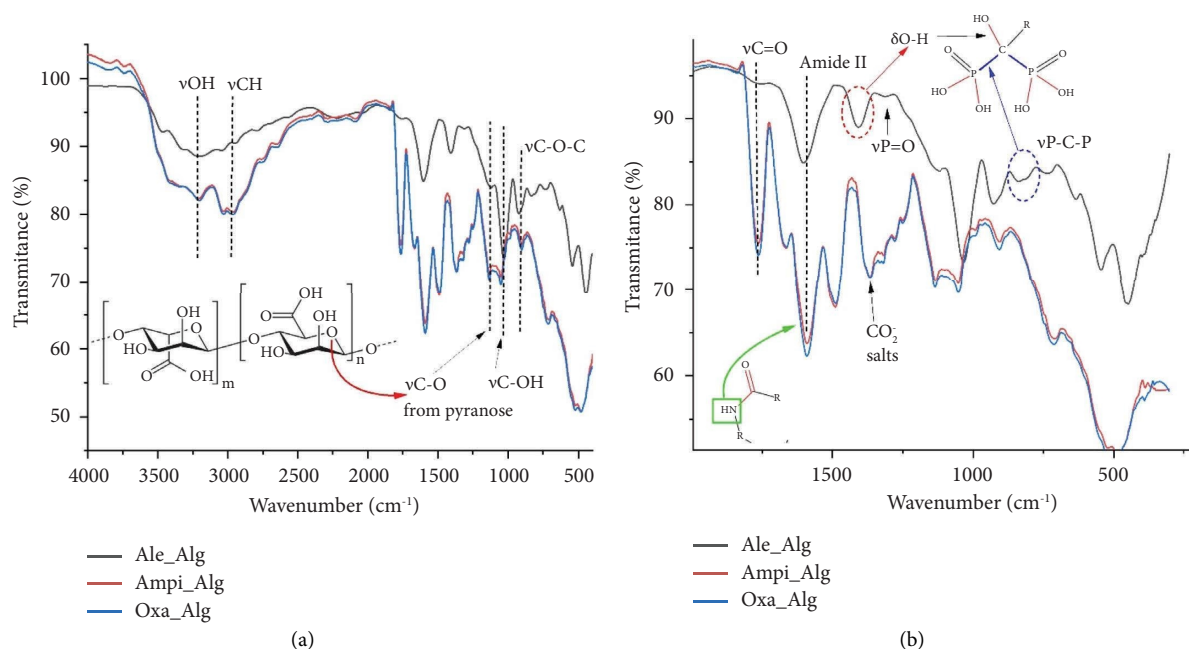


FIGURE 5: (a) FTIR spectrum of alginate-based membranes with incorporated antibiotic drugs; (b) highlighting the most significant peaks of the active substances.

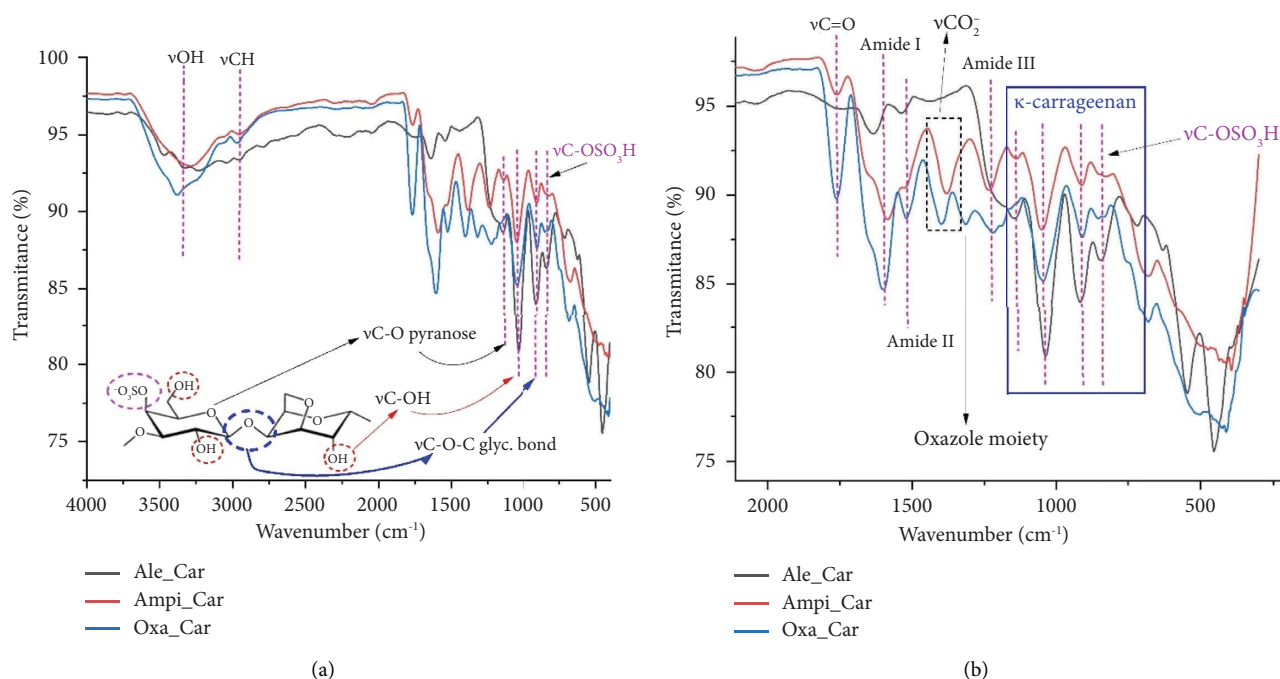


FIGURE 6: (a) FTIR spectrum of κ -carrageenan-based membranes with incorporated antibiotic drugs; (b) peaks that confirm the presence of active substances in studied membranes.

to their successful inclusion in the studied mixtures (Ampi_Chit and Oxa_Chit). Another way to confirm their presence in the studied mixtures is the skeletal vibration of the benzene ring at 1485.78 cm^{-1} and the vibration of the CO_2^- at 1365.05 cm^{-1} (since they are in sodium salt form). All these vibrations are found only in the FTIR spectra of these two lactam antibiotics.

In the case of Alen, an intense peak is located at 1631.24 cm^{-1} , indicating that the terminal amino group is protonated. On a closer look at the peak attributed to the Alen_Chit mixture, we can observe that around the value of 1000 cm^{-1} , which is attributed to the polymer matrix, the intensity of the peaks is much more pronounced because in this wavenumber range, the vibrations of the phosphonic

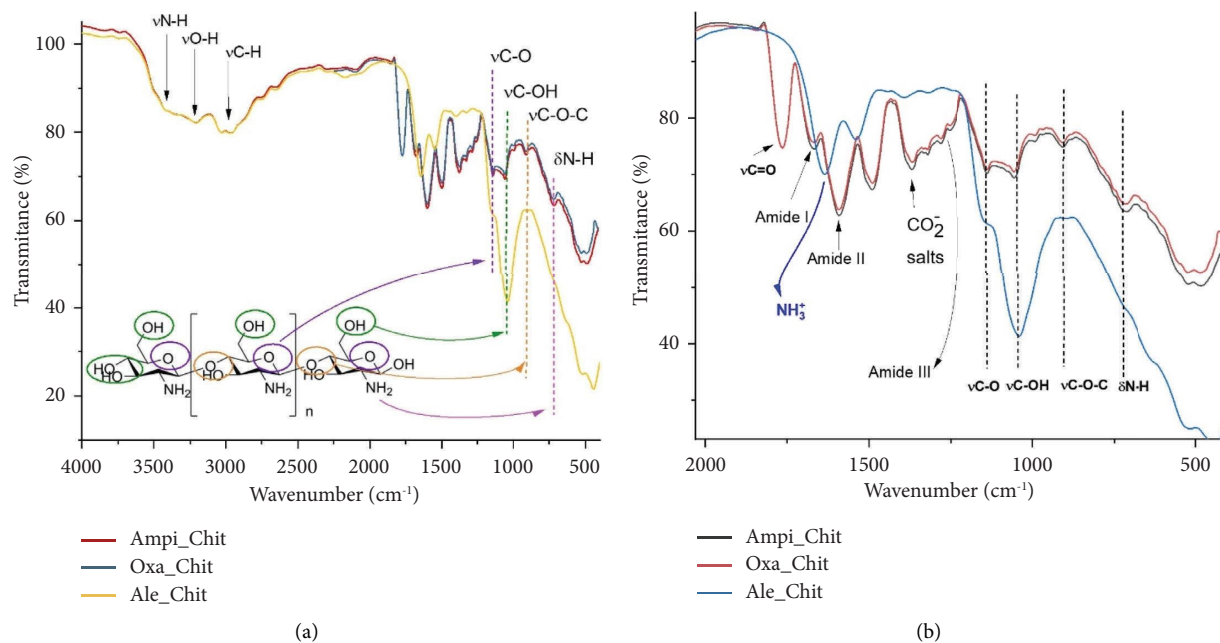


FIGURE 7: (a) FTIR spectrum of chitosan-based membranes with incorporated antibiotic drugs; (b) vibrations that highlight the successful incorporation of active substances.

portion of Alendronate can be found, such as $\nu\text{P}=\text{O}$, $\nu\text{P}-\text{OH}$, and even $\nu\text{P}-\text{C}-\text{P}$ (as mentioned earlier).

3.1.2. FTIR Spectra of Ternary Mixture. The spectra of the ternary mixtures were compared with the spectra of the individual active substances and with the spectra of the binary mixture containing antibiotic and bisphosphonate to determine the integrity of the active substances within the mixtures. Only the important characteristic bands of the active substances are followed.

In the case of ternary mixtures, less distinct peaks of the active substances are observed, an observation that can be justified by the influence of the biopolymer in the mixture and the fact that the active substance is present in a much smaller amount in the mixture.

It can be seen that Chit has a much greater influence in the mixture, which leads us to conclude that there is a slight interaction with the active substances. The presence of Alen is demonstrated in the case of ternary mixtures with Car and Alg by the C-H, N-H, and O-H vibrations in the range of $2950\text{--}3500\text{ cm}^{-1}$ and by the wavenumbers in the range of $1250\text{--}1000\text{ cm}^{-1}$ (Figure 8) but is much weaker or absent in mixtures with Chit.

The characteristic Oxa bands in the range of $1800\text{--}1500\text{ cm}^{-1}$, indicative of the presence of CO-NH and C=O bonds, are better highlighted in the ternary mixtures with Car, Alg and weak or absent in the case of the mixture with Chit.

In Figure 8(a), it can be seen that the bands, characteristic of the active substances Oxa and Alen, are best represented in the case of the mixture with Alg, unlike the other two biopolymers. Figure 8(b) highlights a very good compatibility between Ampri and Alen with Alg and Chit. As for Car, the characteristic bands of the two active substances

are slightly less represented but are visible. The data will be supplemented with UV-Vis studies.

3.1.3. FTIR Spectra of Quaternary Mixture. The FTIR study of the quaternary mixtures was performed to highlight the influence of BON/BOS within the mixtures. It was found in all cases that the BON/BOS type material does not affect the spectrum of the mixtures. Also, in these spectra, it can be suspected that Chit would present interactions with both active substances.

Analyzing the superimposed spectra of quaternary mixtures (Figures 9(a) and 9(b)), the same conclusions can be drawn as in the case of ternary mixtures, namely, the fact that the characteristic bands of Oxa, Ampri, and Alen are best visible in the FTIR spectra of materials containing Alg and Car as biopolymers. It can also be argued that BON and BOS do not interact with the active substances.

According to the FTIR study of the studied mixtures, it can be said that the studied components in the binary mixtures have no interactions. In the ternary and quaternary mixtures (the final materials), interactions between Chi and the two antibiotics were highlighted, which occurred only in the presence of moisture introduced by the biopolymer during the preparation of the final materials.

3.2. Thermal Analysis. Thermal analysis was performed only in the case of binary mixtures to determine possible interactions between components. Thermal analysis was not performed on the other mixtures because the thermal behavior of the active substance is much more difficult to reveal for tertiary and quaternary mixtures, and we consider that the spectroscopic study is sufficient to elucidate and confirm possible interactions between the components.

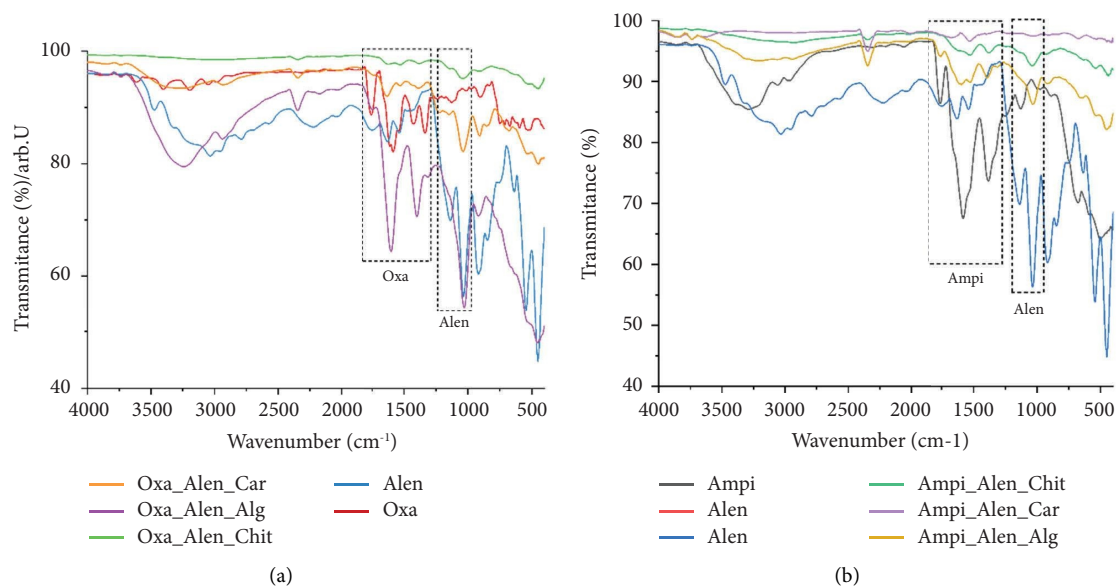


FIGURE 8: (a) Comparative FTIR spectra of ternary mixture with Oxa; (b) comparative FTIR spectra of ternary mixture with Amp.

3.2.1. Thermal Analysis of Active Substances and Binary Mixture. The thermogravimetric study started with the thermal analysis of the two antibiotics and alendronate to highlight the thermal behavior of the active substances.

The study of the thermal analysis of Amp (Figure 10(a)) was carried out under the same conditions and showed that Amp in the mixtures is in the form of amorphous monohydrate I according to the literature [44].

The thermogram of the active substance Amp, which is in the form of amorphous monohydrate, shows an endothermic process corresponding to water loss in the range of 25–190°C, indicating the presence of water molecules in the form of moisture and water in the monohydrate. In the range of 200–500°C, a continuous mass loss is observed, indicating a complex decomposition without being able to separate the processes on the TG curve. Several processes can be observed on the HF curve, namely, an exothermic process with a maximum at 230°C with a loss of 69.26% of the sample mass, followed by an endothermic process with a maximum at 260°C with a loss of 21.58%. The literature suggests that ampicillin monohydrate exhibits a melting process that begins with the decomposition of the sample [36–54].

Analyzing the thermograms of the binary mixtures of Amp with Alg, Car, and Chit (Figure 10(a)), we can support the fact that the inclusion of Amp in the mixture leads to decomposition at lower temperatures, which can be argued by the fact that Amp is present in the mixture in a 1 : 1 ratio. It can also be argued that the biopolymer has a decomposition process in the same range as Amp. It can be seen on the NHF curves of the binary mixtures that the contributions of the two components are combined [50, 51].

Thermal analysis of Oxa (Figure 10(b)) shows a continuous loss of mass beginning at temperatures above 150°C [55]. Several processes are observed on the NHF curve, which leads us to the idea that the decomposition of the

active substance occurs through a complex process. One can observe the presence of an endothermic process with a maximum at 188°C associated with the melting of Oxa. The mass loss in the range of 150–400°C is approximately 60% of the mass of the sample. The thermogravimetric curves of the Oxa-Alg, Oxa-Car, and Oxa-Chit mixtures highlight the thermal decomposition of the active substance Oxa in the same temperature range without the melting process being visible, which can be explained by the fact that the active substance is distributed within polymer mass. It can be observed that both components within the binary mixtures present stages of decomposition in the same temperature range. Therefore, it is difficult to highlight on the NHF curve the individual decomposition processes of Oxa within the mixtures with Car and Chit. In the case of the Oxa-Alg binary mixture, the thermal effects that accompany the decomposition of the active substance can be observed but at slightly higher temperatures.

The thermal analysis of the active substance Alen, shown in Figure 10(c), performed in an atmosphere of synthetic air with a heating rate of 10°C•min⁻¹ up to 500°C, reveals several stages of decomposition in agreement with the data published in previous studies [21, 56].

The first stage of decomposition, between 110°C and 160°C, with a maximum of the reaction rate at 130°C is attributed to the loss of the three water molecules (water of crystallization). The second stage, between 190°C and 289°C, is attributed to the loss of ammonia. The studied compound has a primary amine and an acidic phosphonate group in the same molecule. The decomposition is in the form of a thermal deamination process consisting of two stages, namely, the process of breaking the C–N bond and that of forming the C–O bond (ether type) [21]. The third process, above 289°C, is very complex. It is a continuous mass loss that can be attributed to different stages of thermal degradation that cannot be separated on the TG curve. Regarding

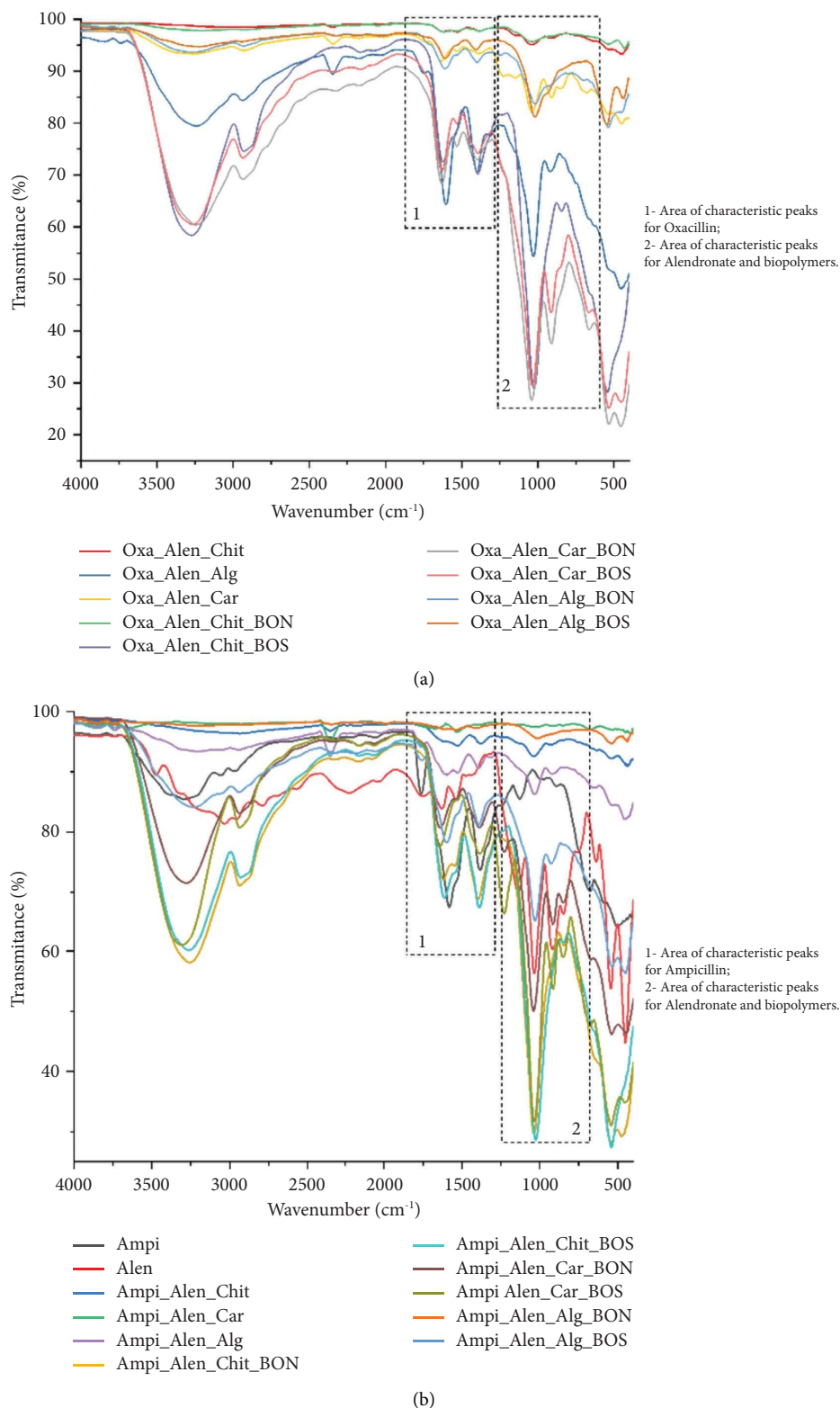


FIGURE 9: (a) Comparative FTIR spectra of quaternary mixture with antibiotics Oxa and Alen. (b) Comparative FTIR spectra of quaternary mixture with antibiotics Ampicillin and Alen.

the thermal analysis of the binary mixtures Alen-Alg, Alen-Car, and Alen-Chit (Figure 10(c)), it can be said that the inclusion of the active substance in the mixture leads to

a shift of the melting point of Alen to lower temperatures which can be argued by the simple presence of Alen in a mixture. The calculated mass losses are in accordance with

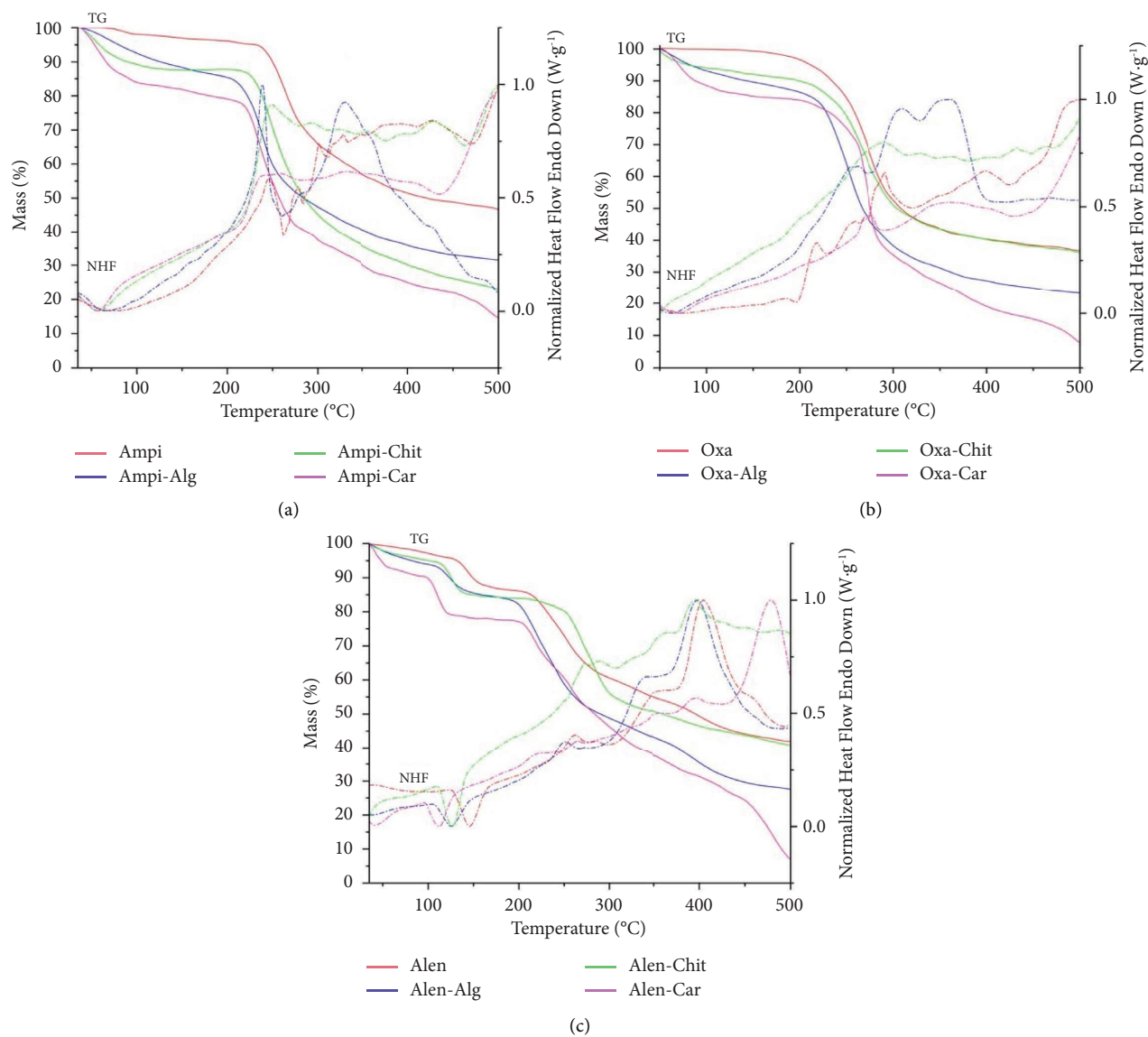


FIGURE 10: (a) Comparative thermoanalytical analysis of Ampicillin with binary mixture Ampicillin-Alg/Car/Chitosan. (b) Comparative thermoanalytical analysis of Oxacillin with binary mixture Oxacillin-Alg/Car/Chitosan. (c) Comparative thermoanalytical analysis of Alendronate with binary mixture Alendronate-Alg/Car/Chitosan.

the mixing ratio of the components within the mixture. The thermogravimetric study of the studied binary mixtures shows the thermal behavior of the components [57], which leads us to conclude that the active substances are present in the binary mixtures. The thermogravimetric study of the other mixtures is too complex to claim that it provides additional data, so we will continue the study with other techniques.

3.3. UV-Vis Analysis of Final Dental Materials. The spectrophotometric analysis (Figures 11(a) and 11(b)) applied to the samples aims to determine the presence or absence of active substances within the final material. Thus, all final materials, i.e., quaternary mixtures, were subjected to this analysis. To confirm the presence of active substances in the obtained membranes using the UV-Vis method, samples of

the materials and active substances (control solutions) were prepared for the antibiotic. For the materials that contained Ampicillin or Oxacillin as antibiotic, 100 mg of the material was weighed and dissolved in 10 ml of distilled water. Since the ratio between the components in each material was 1:6 (antibiotic: Alendronate + biopolymer + BOS/BON), it was determined by calculations that approximately 1.5 mg of the active substance of the antibiotic was present. Therefore, the control solutions of the active substances were prepared to contain the same concentration of antibiotic for Oxacillin and 1:4 for Ampicillin.

The spectra of the samples containing Oxacillin were compared with the spectrum of the standard solution, and the presence of a light absorption band in the UV-Vis spectrum below ~260 nm is observed. The band attributed to the amide $n \rightarrow \pi^*$ transition in the β -lactam ring is present at

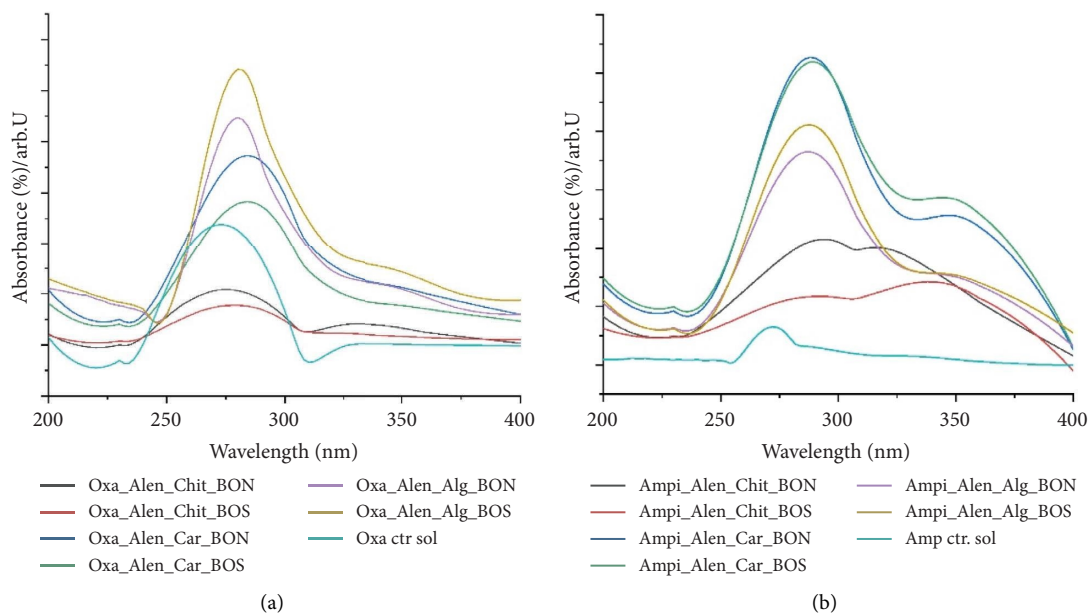


FIGURE 11: (a) UV-Vis spectrum for Oxa control solution and final materials with Oxa; (b) UV-Vis spectrum for Ampicillin control solution and final materials with Ampicillin.

230 nm, and the band due to the aromatic $\pi \rightarrow \pi^*$ transition is present as a shoulder around 270 nm [58].

The band at 270 nm is found with the same intensity and at a slightly higher wavelength in the case of materials based on Car and Alg with BON or BOS. The same cannot be said for materials that have Chit as a biopolymer. In the case of Chit-based materials, the absorption band appears at 270 nm but less intense, which leads us to the idea supported by the other results of a partial interaction between Chit and Oxa.

When the spectra of the samples containing Ampicillin are compared with those of the standard solution of Ampicillin as control samples, the same absorption maximum at 268 nm due to the aromatic transition type $\pi \rightarrow \pi^*$ is observed for the analyzed materials, except for the materials containing Chit as a biopolymer. Thus, we can say that Chit shows interactions with the analyzed antibiotics in the materials synthesized in this study.

In conclusion, we can say that the active substance is present in the matrix of the materials based on Car and Alg and does not interact with the other components of the materials.

3.4. SEM_EDX Analysis. The study of the final materials by the SEM-EDX analysis began with the analysis of the two variants currently used in dentistry, the synthetic BOS and the natural BON (Figure 12).

The SEM analysis (Figure 13) of the two bones used shows a different aspect, namely, in the case of the natural material BON, particles of different sizes are observed, unlike the synthetic material BOS, where the particles have a similar size. EDS analysis has highlighted the different compositions of the two materials, namely, in the case of BON, there are Na and Mg impurities of almost 3%, and the Ca : P ratio is 1.8. In the case of BOS, the presence of only Mg (0.5%) as an

impurity is observed in a much smaller quantity and the Ca : P ratio is 2.19.

Table 4 shows schematically the results obtained in the case of the EDS study of the final materials. The data presented refer only to the composition in Ca, P, O, Na, and Mg. It is observed that in the case of samples containing BON, the percentage of P is lower than in the case of samples with BOS, which derives from the composition of the Bio-Oss source. Comparing the SEM analyses of the final materials, we can observe that the materials containing BOS are more homogeneous and we can also observe that the final materials have a different appearance if they have BON or BOS in their composition. The materials that contain Chit as a biopolymer have a completely different appearance in terms of homogeneity and crystallization of the active substances.

According to the FTIR, thermogravimetry, UV-Vis, and SEM analyses performed in this study, it can be said that it is quite easy to obtain materials that can be used in dental practice with multiple roles, namely, materials that facilitate bone reconstruction through the local administration of bisphosphonate, the calcium source as well as the antibiotic.

Administration is efficient in the case of both active substances avoiding Chit as a biopolymeric material. The choice of antibiotic can be made by the doctor depending on medical considerations. The active substances can be administered in a way that limits adverse effects and maximizes local beneficial effects.

3.5. Cytotoxicity/Biocompatibility Test. The MCF7 cell line was used for the cytotoxicity/biocompatibility assay. Cell proliferation was determined using the Alamar Blue assay [59]. Materials validated from a physical-chemical point of view were used in these tests, namely, the samples

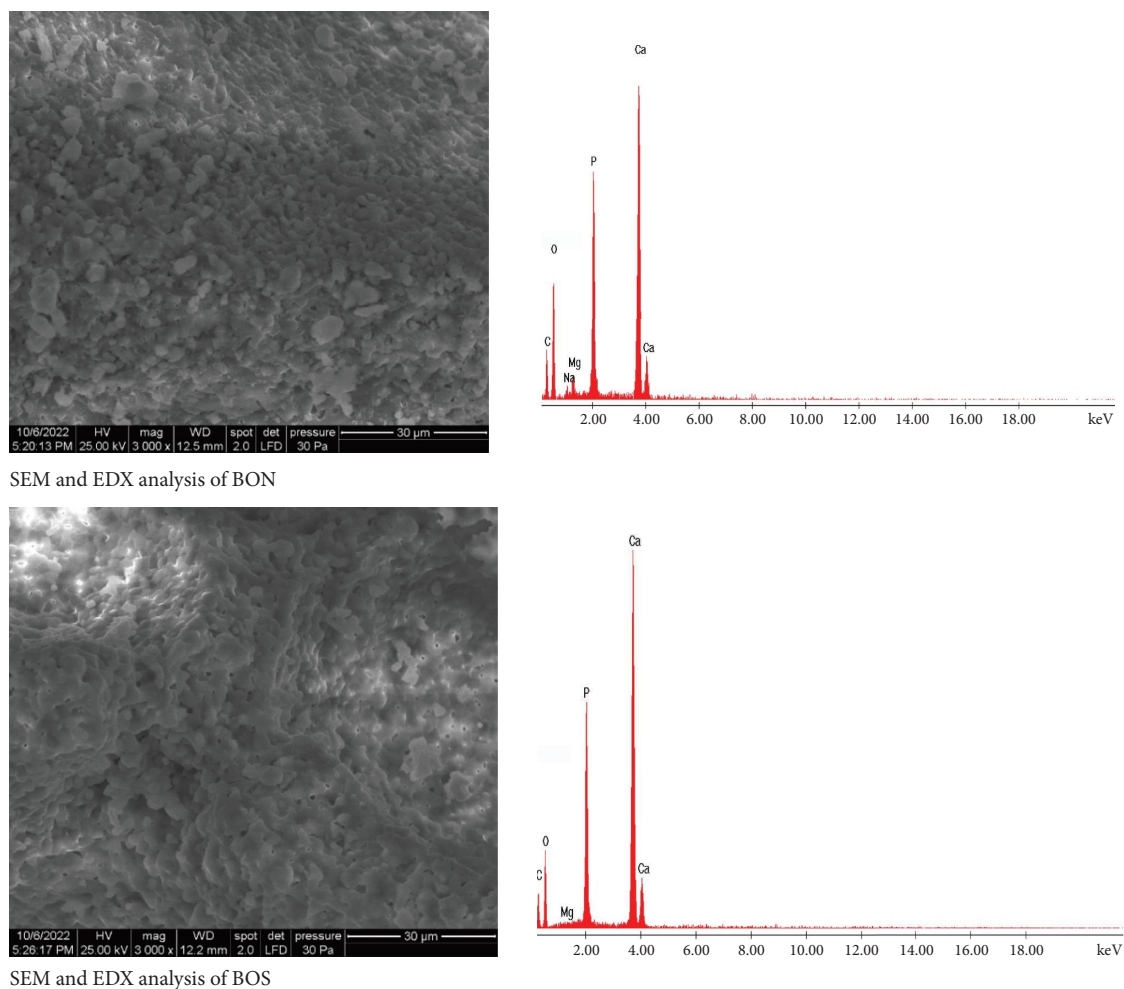


FIGURE 12: SEM and EDS analysis of BON and BOS.

Oxa_Alen_Car (1), Amp_i_Alen_Car (2), Oxa_Alen_Alg (3), and Amp_i_Alen_Alg (4). BON and BOS were excluded due to solubility problems. BON and BOS are materials whose cytotoxicity is known and are materials currently used in

dental practice. All assays were performed three times for each sample. To calculate the inhibition index, the following formula was used:

$$\text{inhibition (\%)} = 100 - \frac{\{[(O2 * A1) - (O1 * A2)] / [(O2 * P1) - (O1 * P2)]\}}{100} \quad (1)$$

O1 = molar extinction coefficient (E) of oxidized Alamar Blue (blue) at 570 nm; O2 = molar extinction coefficient (E) of oxidized Alamar Blue at 600 nm; A1 = absorbance of tested well at 570 nm; A2 = absorbance of tested well at 600 nm; P1 = absorbance of positive growth control well (cells and Alamar Blue but no test agent) at 570 nm; P2 = absorbance of positive growth control well (cells and Alamar Blue but no test agent) at 600 nm.

The cell proliferation rate was evaluated by applying the Alamar blue assay, in which the extinction values were read 24, 48, and 72 hours after the application of the solutions of the compounds of interest. The results are expressed in percent.

In the case of cells exposed to the C1 concentration, compound (1) determined a moderate inhibition of cell proliferation, with slight variations depending on the exposure time. In this case, the average inhibition being 43.47% for the 24 h incubation, 32.43% for the 48 h exposure, and, respectively, 36.65% for the 72 h incubation of the cells with compound (1). For C2–C5 concentrations, we noticed a minor increase in cell inhibition, between 21.43% (C4) and 9.8% (C5). Incubation of cells with compound 1, for 48 h and 72 h, determined the stimulation of cell proliferation, independent of the duration of exposure, marked by negative values of the inhibition rate (Figure 14).

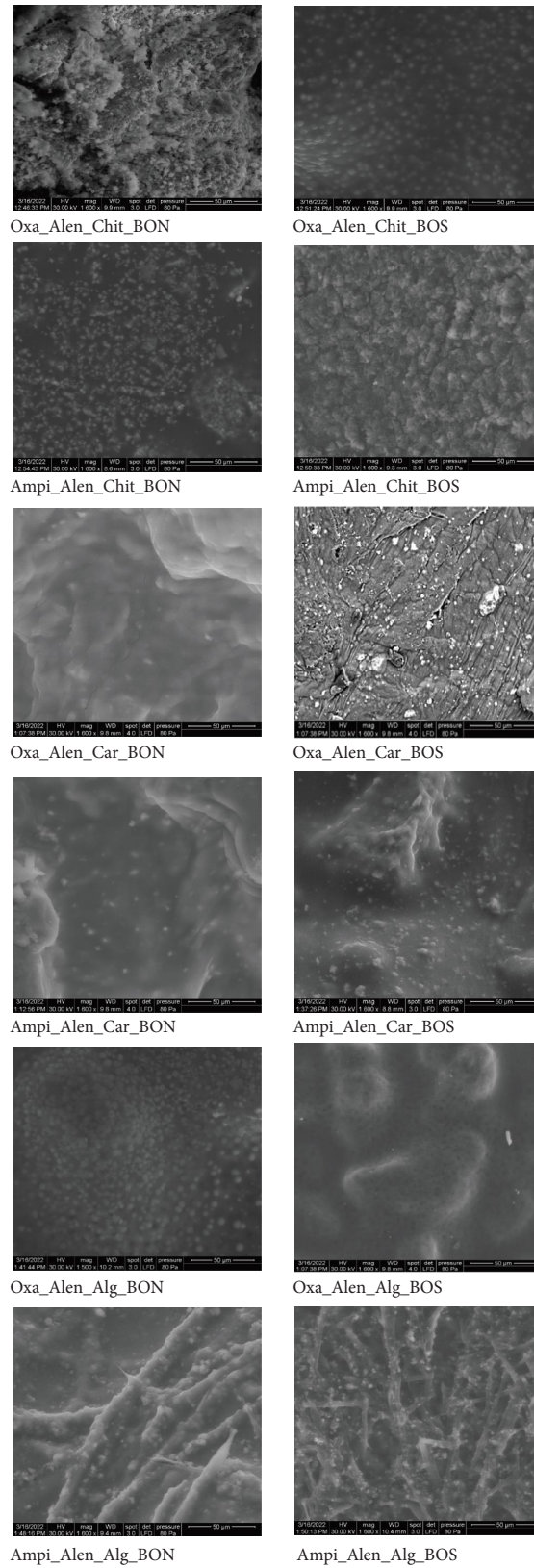


FIGURE 13: SEM analysis of final materials with antibiotics, Alen, and BON or BOS.

TABLE 4: The results of the EDS study in the case of the final materials.

Samples	Element wt (%)				
	Ca	P	O	Na	Mg
Oxa_Alen_Chit_BON	1.64 ± 0.10	6.93 ± 0.15	40.21 ± 0.61	4.91 ± 0.15	0.52 ± 0.05
Oxa_Alen_Chit_BOS	0.99 ± 0.09	10.86 ± 0.28	33.01 ± 0.58	9.33 ± 0.21	1.41 ± 0.08
Ampi_Alen_Chit_BON	1.63 ± 0.08	8.36 ± 0.13	34.27 ± 0.46	4.23 ± 0.10	0.59 ± 0.04
Ampi_Alen_Chit_BOS	1.08 ± 0.07	11.42 ± 0.16	31.94 ± 0.47	4.19 ± 0.11	
Oxa_Alen_Car_BON	1.62 ± 0.08	10.38 ± 0.21	43.25 ± 0.47	6.88 ± 0.14	
Oxa_Alen_Car_BOS	1.06 ± 0.03	11.26 ± 0.14	33.72 ± 0.45	1.12 ± 0.05	0.15 ± 0.02
Ampi_Alen_Car_BON	1.08 ± 0.06	4.38 ± 0.08	33.87 ± 0.44	2.65 ± 0.08	
Ampi_Alen_Car_BOS	1.03 ± 0.07	1.27 ± 0.05	31.38 ± 0.46	3.44 ± 0.09	
Oxa_Alen_Alg_BON	1.19 ± 0.07	6.98 ± 0.13	34.92 ± 0.49	5.65 ± 0.13	0.39 ± 0.03
Oxa_Alen_Alg_BOS	2.25 ± 0.08	10.73 ± 0.13	46.07 ± 0.41	4.09 ± 0.09	1.19 ± 0.05
Ampi_Alen_Alg_BON	0.79 ± 0.08	6.67 ± 0.16	32.95 ± 0.58	10.19 ± 0.21	0.31 ± 0.04
Ampi_Alen_Alg_BOS	0.96 ± 0.19	10.30 ± 0.19	40.77 ± 0.49	5.38 ± 0.12	

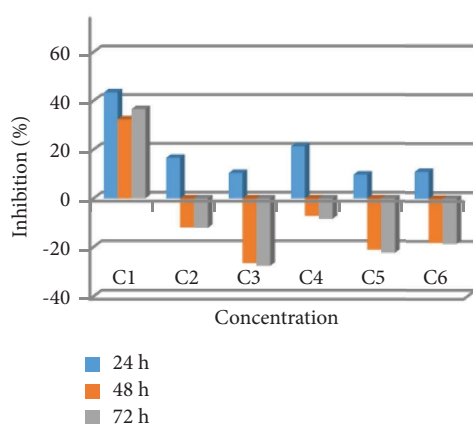


FIGURE 14: Inhibition rate of cell proliferation incubated with compound (1) Oxa_Alen_Car.

In the case of compound (2), increased inhibition of the cellular development rate was observed at 1% concentration for all incubation times (48.08% at 24 hours, 38.01% at 48 hours, and 50.05% at 72 hours). Also, exposure of MCF7 cells to C2 concentration (0.5%) for 24 hours resulted in an increase in cell inhibition of 42.43% and cell inhibition rate of 26.23% and 29.42% for 48 and 72 hours exposure. An insignificant increase in the inhibition rate (less than 10%) was observed when cells were treated with compound (2) at C3-C6 concentrations for 48 and 72 hours, while 24-hour exposure determined a change in cell inhibition at percentages of 21.57% (C3), 27.18% (C4), 21.37% (C5), and 13% (C6) (Figure 15).

For the third compound (3), we observed a decrease in the inhibition rate as a function of exposure time when incubated with concentrations between C1 and C3. For C1, when cells were incubated with this compound for a longer period of time (72 hours), significant inhibition of cell culture development was observed, with an inhibition rate of 68.79%. For the other C2 and C3 concentrations, the inhibition was moderate, with rates ranging from 25 to 45%. For the 24h exposure, the highest rate of inhibition was observed for C6. For C4 and C5, the values of inhibition rate

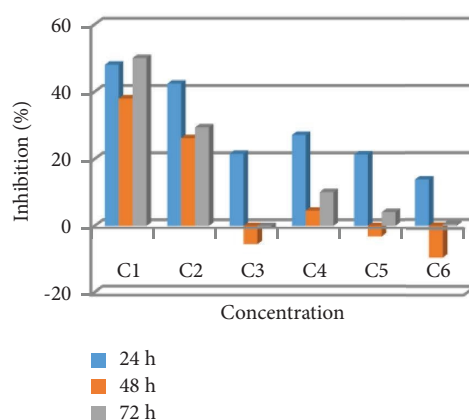


FIGURE 15: Inhibition rate of cell proliferation incubated with compound (2) Amp_i_Alen_Car.

are under 6%. For a longer exposure time, proliferation of cells was observed for C4 and C5 (Figure 16).

Exposure of MCF7 cells to compound (4) resulted in a significant reduction in cell growth, with the IC50 index (concentration causing a reduction in the cell proliferation rate of at least 50%) achieved at 24 h exposure for C1. At the 48- and 72-hour exposures for the same concentration, the inhibition rate was between 40 and 45%. For the other C2-C6 concentrations, we observed lower inhibition at the 24-h incubation. At 48 and 72 hours after exposure, the cell inhibition rate was insignificantly reduced or, on the contrary, stimulated (Figure 17).

Although no linear dependence was observed in relation to the applied dose, the highest inhibition rate was observed when C1 concentrations were administered (1%) for all tested compounds. The other concentrations determined a moderate inhibition of cell growth. Instead, at some concentrations, a stimulation of the proliferative process was observed. The IC 50 index was reached in the case of the C1 concentration of compound (4), which indicates the cytotoxic nature of the 1% concentration of this compound. In conclusion, compounds (1) and (4) proved to be biocompatible at concentrations between 0.5% and 0.03125%, for incubation over a longer period of time, of 48 h and 72 h,

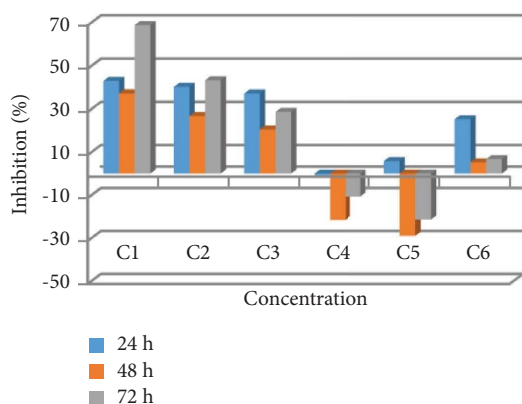


FIGURE 16: Inhibition rate of cell proliferation incubated with compound (3) Oxa_Alen_Alq.

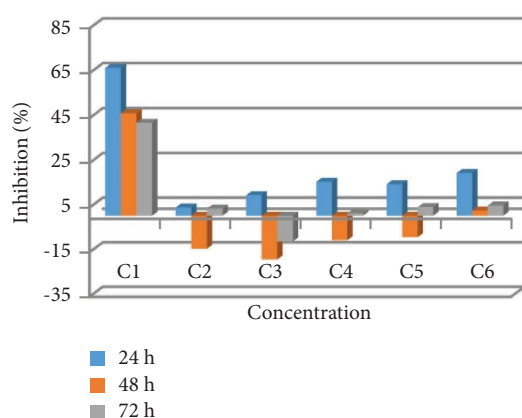


FIGURE 17: Inhibition rate of cell proliferation incubated with compound (4) Ampi_Alen_Alq.

respectively. The highest proliferation rate was noticed in case of both compounds for C3 (0.25%).

4. Conclusions

In dental practice, BON and BOS are materials currently used for bone reconstruction. Similarly, Alen is used to facilitate bone synthesis through oral administration and antibiotic treatment is also used in dentistry to prevent or treat local infections.

As a result of this study, it was possible to obtain and physicochemically characterize several materials combining antibiotics, bisphosphonate and Ca sources.

Although Car and Alg have been widely used in recent years as carriers for different active substances in different drug delivery systems, this study demonstrates a new method that can lead to a complex local drug delivery system.

The IR spectra of the analyzed final materials show peaks characteristic of the functional groups of the active substances and characteristic peaks of the biopolymer and of BON/BOS. The FTIR study showed that all the active substances are present intact in the mixtures with Car and Alg as biopolymer and the materials with Chit as biopolymer are invalid.

The UV-Vis analysis confirmed the results of the FTIR spectra and thermogravimetric analyses.

The TG analysis showed good thermal stability in the temperature range of 25–170°C for both the final materials and the incorporated active substances.

Thermal analysis argued the presence of active substances in intact form in the binary mixtures but did not provide clear data in the case of the ternary and quaternary mixtures.

The present study succeeds by combining the results of several complementary physicochemical techniques (TG, FTIR, scanning electron microscopy with SEM, and UV-Vis ultraviolet-visible), the validation of materials suitable for medical use for stimulation bone reconstruction together with the administration of a quantity lower than antibiotic and alendronate, thus avoiding the side effects that occur in some patients in case of oral or injectable administration. The validation had in mind the establishment of materials that do not present interactions between the medicinal substances studied and that can later be tested in vitro or in vivo. The results of the cytotoxicity test showed increased biocompatibility for compounds 1 and 4 at concentrations between 0.5% and 0.03125%, when incubated for prolonged periods of 48 h and 72 h, especially for 0.25% concentration.

According to the FTIR, thermogravimetry, UV-Vis, and SEM analyses performed in this study, it can be said that it is quite easy to obtain materials that can be used in dental practice with multiple roles, namely, materials that facilitate bone reconstruction through the local administration of bisphosphonate and the calcium source, as well as the antibiotic.

Administration is efficient in the case of both active substances avoiding Caras a biopolymeric material. The choice of antibiotic can be made by the doctor depending on medical considerations. The active substances can be administered in a way that limits adverse effects and maximizes local beneficial effects.

Data Availability

All data used to support the findings of this study are included in the article.

Conflicts of Interest

There are no conflicts of interest between the co-authors.

Authors' Contributions

Conceptualization was performed by G.V., D.N., D.O., A.M., A.G., and D.J.; data curation was conducted by D.O., T.V., I-A.B., A.T., N.C., R.P., and G.V.; formal analysis was conducted by G.V., P.S., D.N., A.P., and T.V.; funding acquisition was carried out by T.V.; investigation was done by G.V., D.O., M.M.B., A.T., and T.V.; methodology was prepared by G.V., I-A.B., D.O., and T.V.; project administration was performed by T.V.; software was handled by T.V. and D.O.; supervision was done by G.V. and T.V.; validation was done by T.V. and G.V.; visualization was performed by

M.M.B., A.M., G.V., and T.V.; writing of the original draft was conducted by D.O., G.V., and T.V., writing, review, and editing were performed by G.V., M.M.B., A.P., and T.V. All authors have read and agreed to the published version of the manuscript. Daniel Negru and Mihaela Maria Budiul are equal contributor as first author.

Acknowledgments

This study was financially supported by personal fundings.

References

- [1] G. A. Abeer, A. A. Fatin, A. N. Abdurahman, A. J. Jhon, and S. A. Hamdan, "A combination of biphasic calcium phosphate (Maxresorb®) and hyaluronic acid gel (Hyadent®) for repairing osseous defects in a rat model," *Applied Sciences*, vol. 10, no. 1, pp. 1–12, 2020.
- [2] J. Zhang, S. Ma, Z. Liu et al., "Guided bone regeneration with asymmetric collagen-chitosan membranes containing aspirin-loaded chitosan nanoparticles," *International Journal of Nanomedicine*, vol. 12, pp. 8855–8866, 2017.
- [3] M. M. Budiul, G. Vlase, D. Negru et al., "Financial inclusion as a fairness criterion in credit risk assessment," 2023, https://papers.ssrn.com/sol3/papers.cfm?abstract_id=4462329.
- [4] D. Okolišan, G. Vlase, T. Vlase, and C. Avram, "Preliminary study of κ -carrageenan based membranes for anti-inflammatory drug delivery," *Polymers*, vol. 14, no. 20, p. 4275, 2022.
- [5] M. Mateescu, G. Vlase, M. M. Budiul, B. D. Cernuşcă, and T. Vlase, "Preliminary study for preparation and characterization of medicated jelly based on Ibuprofen or Ambroxol," *Journal of Thermal Analysis and Calorimetry*, vol. 148, no. 10, pp. 4601–4614, 2023.
- [6] S. Schafer, H. Al-Qaddo, M. Gosau et al., "Cytocompatibility of bone substitute materials and membranes," *In Vivo*, vol. 35, no. 4, pp. 2035–2040, 2021.
- [7] N. V. M. Milhan, I. C. S. Carvalho, R. F. Prado, E. D. S. Trichês, C. H. R. Camargo, and S. E. A. Camargo, "Analysis of indicators of osteogenesis, cytotoxicity and genotoxicity of an experimental β -TCP compared to other bone substitutes," *Acta Scientiarum Health Sciences*, vol. 39, no. 1, pp. 97–105, 2017.
- [8] O. Holte, E. Onsøyen, R. Myrvold, and J. Karlsen, "Sustained release of water-soluble drug from directly compressed alginate tablets," *European Journal of Pharmaceutical Sciences*, vol. 20, no. 4–5, pp. 403–407, 2003.
- [9] H. A. Salih and M. A. A. Faiza, "The effect of incorporation kappa-carrageenan powder on the physical and mechanical properties of the heat-cured acrylic-based soft denture lining material in clinical use," *Indian Journal of Forensic Medicine and Toxicology*, vol. 14, pp. 1770–1778, 2020.
- [10] C. D. C. Spadari, F. W. M. D. S. de Bastiani, L. B. Lopes, and K. Ishida, "Alginate nanoparticles as non-toxic delivery system for miltefosine in the treatment of candidiasis and cryptococcosis," *International Journal of Nanomedicine*, vol. 14, pp. 5187–5199, 2019.
- [11] M. Croes, B. C. H. van der Wal, and H. C. Vogely, "Impact of bacterial infections on osteogenesis: evidence from in vivo studies," *Journal of Orthopaedic Research*, vol. 37, no. 10, pp. 2067–2076, 2019.
- [12] C. Celesti, D. Iannazzo, C. Espro et al., "Chitosan/POSS hybrid hydrogels for bone tissue engineering," *Materials*, vol. 15, no. 22, p. 8208, 2022.
- [13] S. Husain, K. H. Al-Samadani, S. Najeeb et al., "Chitosan biomaterials for current and potential dental applications," *Materials*, vol. 10, no. 6, p. 602, 2017.
- [14] D. G. Miranda, S. M. Malmonge, D. M. Campos, N. G. Attik, B. Grosogeat, and K. Gritsch, "A chitosan-hyaluronic acid hydrogel scaffold for periodontal tissue engineering," *Journal of Biomedical Materials Research Part B: Applied Biomaterials*, vol. 104, no. 8, pp. 1691–1702, 2016.
- [15] M. Abdel Mouez, N. M. Zaki, S. Mansour, and A. S. Geneidi, "Bioavailability enhancement of verapamil HCl via intranasal chitosan microspheres," *European Journal of Pharmaceutical Sciences*, vol. 51, pp. 59–66, 2014.
- [16] J. M. Oliveira, M. T. Rodrigues, S. S. Silva et al., "Novel hydroxyapatite/chitosan bilayered scaffold for osteochondral tissue-engineering applications: scaffold design and its performance when seeded with goat bone marrow stromal cells," *Biomaterials*, vol. 27, no. 36, pp. 6123–6137, 2006.
- [17] P. Chavanne, S. Stevanovic, A. Wüthrich et al., "3D printed chitosan/hydroxyapatite scaffolds for potential use in regenerative medicine," *Biomedizinische Technik Biomedical engineering*, vol. 58, no. Suppl 1, 2013.
- [18] S. B. Qasim, S. Najeeb, R. M. Delaine-Smith, A. Rawlinson, and I. Ur Rehman, "Potential of electrospun chitosan fibers as a surface layer in functionally graded GTR membrane for periodontal regeneration," *Dental Materials*, vol. 33, no. 1, pp. 71–83, 2017.
- [19] H. J. Haugen, P. Basu, M. Sukul, J. F. Mano, and J. E. Reseland, "Injectable biomaterials for dental tissue regeneration," *International Journal of Molecular Sciences*, vol. 21, no. 10, p. 3442, 2020.
- [20] C. J. G. Abrego, L. Dedroog, O. Deschaume et al., "Multiscale characterization of the mechanical properties of fibrin and polyethylene glycol (PEG) hydrogels for tissue engineering applications," *Macromolecular Chemistry and Physics*, vol. 223, no. 1, p. 2022, 2022.
- [21] A. Bascones Martínez, J. M. Aguirre Urizar, A. Bermejo Fenoll et al., "Consensus statement on antimicrobial treatment of odontogenic bacterial infections," *Medicina Oral, Patología Oral, Cirugía Bucal*, vol. 9, no. 5, pp. 369–376, 2004.
- [22] C. Z. Koyuncuoglu, M. Aydin, N. I. Kirmizi et al., "Rational use of medicine in dentistry: do dentists prescribe antibiotics in appropriate indications," *European Journal of Clinical Pharmacology*, vol. 73, no. 8, pp. 1027–1032, 2017.
- [23] K. C. Wade and D. K. Benjamin Jr, "CHAPTER 37- clinical pharmacology of anti-infective drugs," *Infectious Diseases of the Fetus and Newborn*, pp. 1160–1211, Saunders elsevier, Philadelphia, PA, USA, Seventh edition, 2011.
- [24] S. C. Sharon, "xPharm: the comprehensive pharmacology reference," 2007, <https://www.sciencedirect.com/topics/biochemistry-genetics-and-molecular-biology/ampicillin>.
- [25] M. Neuville, N. El-Helali, E. Magalhaes et al., "Systematic overdosing of oxa- and cloxacillin in severe infections treated in ICU: risk factors and side effects," *Annals of Intensive Care*, vol. 7, no. 1, p. 34, 2017.
- [26] S. C. Doca, P. Albu, I. Ceban, A. Anghel, G. Vlase, and T. Vlase, "Sodium alendronate used in bone treatment: a complex study on the thermal behavior of the bioactive compound and its binary mixture with several excipients," *Journal of Thermal Analysis and Calorimetry*, vol. 126, no. 1, pp. 189–194, 2016.

- [27] S. J. Meraw, C. M. Reeve, and P. C. Wollan, "Use of alendronate in peri-implant defect regeneration," *Journal of Periodontology*, vol. 70, no. 2, pp. 151–158, 1999.
- [28] L. Levin, E. C. Bryson, D. Caplan, and M. Trope, "Effect of topical alendronate on root resorption of dried replanted dog teeth," *Dental Traumatology*, vol. 17, no. 3, pp. 120–126, 2001.
- [29] N. Malden, C. Beltes, and V. Lopes, "Dental extractions and bisphosphonates: the assessment, consent and management, a proposed algorithm," *British Dental Journal*, vol. 206, no. 2, pp. 93–98, 2009.
- [30] S. Kalra and V. Jain, "Dental complications and management of patients on bisphosphonate therapy: a review article," *Journal of Oral Biology and Craniofacial Research*, vol. 3, no. 1, pp. 25–30, 2013.
- [31] S. Kuhl, C. Walter, S. Acham, R. Pfeffer, and J. T. Lambrecht, "Bisphosphonate-related osteonecrosis of the jaws- A review," *Oral Oncology*, vol. 48, no. 10, pp. 938–947, 2012.
- [32] I. Coskun Benlidayi and R. Guzel, "Oral bisphosphonate related osteonecrosis of the jaw: a challenging adverse effect," *ISRN Rheumatology*, vol. 2013, pp. 1–6, 2013.
- [33] N. B. Watts and D. L. Diab, "Long-term use of bisphosphonates in osteoporosis," *Journal of Clinical Endocrinology and Metabolism*, vol. 95, no. 4, pp. 1555–1565, 2010.
- [34] R. E. Coleman and E. V. McCloskey, "Bisphosphonates in oncology," *Bone*, vol. 49, no. 1, pp. 71–76, 2011.
- [35] O. I. Balean, A. D. Floare, R. Focht et al., "Comparative effects of oral and injectable bisphosphonates in primary human gingival fibroblasts," *Revista de Chimie*, vol. 70, no. 9, pp. 3325–3329, 2019.
- [36] S. J. Meraw and C. M. Reeve, "Qualitative analysis of peripheral peri-implant bone and influence of alendronate sodium on early bone regeneration," *Journal of Periodontology*, vol. 70, no. 10, pp. 1228–1233, 1999.
- [37] C. A. Marioane, M. Bunoiu, M. Mateescu, P. Sfirloagă, G. Vlase, and T. Vlase, "Preliminary study for the preparation of transmucosal or transdermal patches with acyclovir and lidocaine," *Polymers*, vol. 13, no. 20, p. 3596, 2021.
- [38] G. Vlase, M. Budiul, T. Vlase, P. Albu, and A. Ledeti, "Thermally induced interactions between adamantan-2-one and some pharmaceutical excipients," *Journal of Thermal Analysis and Calorimetry*, vol. 131, no. 1, pp. 201–213, 2018.
- [39] M. Budiul, P. Albu, G. Vlase, V. Turcuş, and T. Vlase, "Thermogravimetric and calorimetric studies performed on memantine hydrochloride to determine its thermal behaviour and possible drug–excipient interactions," *Journal of Thermal Analysis and Calorimetry*, vol. 127, no. 1, pp. 555–564, 2017.
- [40] M. Mateescu, M. Budiul, P. Albu, G. Vlase, and T. Vlase, "Thermal behavior and kinetic study of degradation for adamantan-2-one versus memantine hydrochloride," *Journal of Thermal Analysis and Calorimetry*, vol. 130, no. 1, pp. 391–396, 2017.
- [41] G. Vlase, M. Budiul, C. Pătruşescu, P. Albu, and T. Vlase, "An extensive compatibility study of mycophenolate mofetil with different excipients by spectroscopic and thermoanalytical investigation techniques," *Journal of Thermal Analysis and Calorimetry*, vol. 131, no. 1, pp. 225–236, 2018.
- [42] P. Albu, M. Budiul, M. Mateescu, V. Chiriac, G. Vlase, and T. Vlase, "Studies regarding the induced thermal degradation, kinetic analysis and possible interactions with various excipients of an osseointegration agent – zoledronic acid," *Journal of Thermal Analysis and Calorimetry*, vol. 130, no. 1, pp. 403–411, 2017.
- [43] I. Ledeti, M. Budiul, P. Matusz et al., "Preformulation studies for nortriptyline: solid-state compatibility with pharmaceutical excipients," *Journal of Thermal Analysis and Calorimetry*, vol. 131, no. 1, pp. 191–199, 2018.
- [44] I. Ledeti, M. Romanescu, D. Circioban et al., "Stability and compatibility studies of levothyroxine sodium in solid binary systems—instrumental screening," *Pharmaceutics*, vol. 12, no. 1, p. 58, 2020.
- [45] R. K. Mishra, P. Mishra, K. Verma et al., "Electrospinning production of nanofibrous membranes," *Environmental Chemistry Letters*, vol. 17, no. 2, pp. 767–800, 2019.
- [46] A. U. Chaudhry, S. P. Lonkar, R. G. Chudhary, A. Mabrouk, and A. A. Abdala, "Thermal, electrical, and mechanical properties of highly filled HDPE/graphite nanoplatelets composites," *Materials Today: Proceedings*, vol. 29, pp. 704–708, 2020.
- [47] N. B. Singh, M. A. Bin Hasan Susan, and R. G. Chaudhary, *Applications of Emerging Nanomaterials and Nanotechnology*, vol. 148, Materials Research Forum LLC, Millersville, PA, USA, 2023.
- [48] V. N. Sonkusare, R. G. Chaudhary, G. S. Bhusari, A. R. Rai, and H. D. Juneja, "Microwave-mediated synthesis, photocatalytic degradation and antibacterial activity of α -Bi₂O₃ microflowers/novel γ -Bi₂O₃ microspindles," *Nano-Structures and Nano-Objects*, vol. 13, pp. 121–131, 2018.
- [49] N. A. Nikonenko, D. K. Buslov, N. I. Sushko, and R. G. Zhabankov, "Spectroscopic manifestation of stretching vibrations of glycosidic linkage in polysaccharides," *Journal of Molecular Structure*, vol. 752, no. 1–3, pp. 20–24, 2005.
- [50] R. G. Chaudhary, P. Ali, N. V. Gandhare, J. A. Tanna, and H. D. Juneja, "Thermal decomposition kinetics of some transition metal coordination polymers of fumaroylbis (paramethoxyphenylcarbamide) using DTG/DTA techniques," *Arabian Journal of Chemistry*, vol. 12, no. 7, pp. 1070–1082, 2019.
- [51] R. G. Chaudhary, H. D. Juneja, and M. P. Gharpure, "Chelate polymer compounds with bis(bidentate) ligand: synthesis, spectral, morphological and thermal degradation studies," *Journal of the Chinese Advanced Materials Society*, vol. 1, no. 2, pp. 121–133, 2013.
- [52] S. Klick, P. G. Muijselaar, J. Waterval et al., "Toward a generic approach for stress testing of drug substances and drug products," *Pharmaceutical Technology*, vol. 29, 2005.
- [53] D. W. Reynolds, K. L. Facchine, J. F. Mullaney, K. M. Alsante, T. D. Hatajik, and M. G. Motto, "Available guidance and best practices for conducting forced degradation studies," *Pharmaceutical Technology*, vol. 26, no. 2, pp. 48–56, 2002.
- [54] C. Baraldi, A. Tinti, S. Ottani, and M. C. Gamberini, "Characterization of polymorphic ampicillin forms," *Journal of Pharmaceutical and Biomedical Analysis*, vol. 100, pp. 329–340, 2014.
- [55] F. Rodante, S. Vecchio, and M. Tomassetti, "Multi-step decomposition processes for some antibiotics," *Thermochimica Acta*, vol. 394, no. 1–2, pp. 7–18, 2002.

- [56] P. Albu, S. C. Doca, A. Anghel, G. Vlase, and T. Vlase, "Thermal behavior of sodium alendronate: a kinetic study under non-isothermal conditions," *Journal of Thermal Analysis and Calorimetry*, vol. 127, no. 1, pp. 571–576, 2017.
- [57] I. Ledeti, G. Vlase, T. Vlase, L. M. Şuta, A. Todea, and A. Fuliaş, "Selection of solid-state excipients for simvastatin dosage forms through thermal and nonthermal techniques," *Journal of Thermal Analysis and Calorimetry*, vol. 121, no. 3, pp. 1093–1102, 2015.
- [58] E. Takács, J. Wang, L. Chu et al., "Elimination of oxacillin, its toxicity and antibacterial activity by using ionizing radiation," *Chemosphere*, vol. 286, no. 1, Article ID 131467, 2022.
- [59] S. N. Rampersad, "Multiple applications of Alamar Blue as an indicator of metabolic function and cellular health in cell viability bioassays," *Sensors (Basel)*, vol. 12, no. 9, pp. 12347–12360, 2012.